13th World Conference on Earthquake Engineering
Vancouver, B.C., Canada
August 1-6, 2004
Paper No. 42

OPTIMAL DESIGN OF SUPPLEMENTAL VISCOUS DAMPERS FOR LINEAR FRAMED STRUCTURES

Oren LAVAN[1] and Robert LEVY[2]

SUMMARY

A methodology for the optimal design of supplemental viscous dampers for framed structures is presented. It addresses the problem of minimizing the added damping subject to a constraint on the maximal interstory drift for an ensemble of realistic ground motion records while assuming linear behavior of the damped structure. The equivalent optimization problem of minimizing the added damping subject to a constraint on the maximal weighted mean square drift is solved instead. The computational effort is appreciably reduced by first solving the optimization problem for one "active" ground motion record. If the resulting optimal design fails to satisfy the constraints for other records from the original ensemble, additional ground motions (loading conditions) are added one by one until the optimum is reached. An efficient selecting process which is presented herein will usually require one or two records to attain an optimum design.

Finally, optimal designs of supplemental dampers are attained for a 2-story shear frame and a 10-story industrial frame for an ensemble of one and twenty time-histories respectively. The resulting viscously damped structures have envelope values of interstory drifts equal or less than the target drifts.

INTRODUCTION

With advances in technology, it appears that the approach to the design of earthquake resisting structures takes a new direction, which allows engineers to design structures for a desired level of seismic protection. Designing structures to behave elastically or near the elastic range during strong ground motions is not economical, and in many cases is not feasible. Therefore enabling the structure to dissipate energy by means of mechanical devices appears very attractive.

A rich variety of energy dissipation devices for passive control may be found in Soong and Dargush [1]. Viscous dampers seem more appropriate in the case of rehabilitation (Miyamoto and Scholl [2]). The

[1] Ph.D. Candidate, Faculty of Civil and Environmental Engineering, Technion - Israel Institute of Technology, Haifa 32000, Israel
[2] Associate professor, Faculty of Civil and Environmental Engineering, Technion - Israel Institute of Technology, Haifa 32000, Israel

main advantage of viscous dampers is that the forces they produce are out of phase with the column's forces due to displacements, and therefore, will not usually require column and foundation strengthening.

Procedures for the design of viscous damping, i.e. their size and distribution, were proposed by several researchers. Constantinou and Tadjbakhsh [3] derived an optimum damping coefficient for a viscous damper placed on the first story of a shear building. Hahn and Sathiavageeswaran [4] investigated the effects of changes in the distribution of added viscoelastic dampers on the response of shear buildings. Zhang and Soong [5] proposed the Sequential Search Algorithm (SSA) for finding the optimal placement of a pre-sized viscoelastic damper based on a controllability index. Application of the SSA algorithm to 3-D torsionally coupled structures and an examination of the effect of ground motion characteristics on the position of the dampers were done by Wu *et al*. [6] Further investigation of the effect of the nature of the excitation using SSA was done by Shukla and Datta [7]. Garcia [8] simplified the SSA algorithm and made it attractive to practicing engineers. Fu [9] and Fu and Kazahiko [10], estimated the damping needed by assuming first mode behavior of the structure and compared the use of viscous and viscoelastic dampers.

Inaudi *et al.* [11] suggested a procedure for minimizing the maximum mean square of steady state drifts under filtered white noise excitation subject to a constraint on the sum of added damping for viscoelastic and friction dampers. Gluck *et al*. [12] proposed several options for finding attained added stiffness and damping matrices based on Riccati's equation. Takewaki [13], Takewaki and Yoshitomi [14] and Takewaki *et al*. [15] suggested a gradient based algorithm for optimal design of viscous damping by minimizing the sum of the amplitudes of the drifts' transfer functions evaluated at the undamped fundamental natural frequency of the structure subject to a constraint on the total added damping. Singh and Moreschi [16] used a gradient based algorithm for the optimal design of viscous and viscoelastic dampers to achieve the best response reduction in structures. They used a non-classically damped response spectrum approach based on a stochastic description of the input motion to evaluate the structural response, and hence the gradients. Singh and Moreschi [17] also used a genetic approach for the optimal design of viscous and viscoelastic dampers to achieve the best response reduction in structures excited by a stationary stochastic input.

The main advantage of using most of these algorithms is the small effort they demand, but a methodology that takes into consideration an optimal design for an ensemble of realistic ground motion records with a specified target performance index is not available.

OPTIMAL PASSIVE CONTROL PROBLEM FORMULATION AND OPTIMIZATION METHODOLOGY

This paper addresses the optimization problem of minimizing the added damping of prelocated dampers subject to a constraint on the maximum interstory drift for a frame excited by an ensemble of realistic ground motion records.

The optimization methodology is based on a repeated solution of an equivalent optimization problem in which the constraint is on the maximum weighted mean square drift rather than the maximum drift itself. The weights are the ratios of the maximal drifts to mean square drifts computed from the previous optimization cycle. The equivalent optimization problem is solved by first deriving the constraint's gradient, and then using an efficient constrained optimization algorithm. In order to reduce computational effort the optimization is first carried out using one "active" ground motion, to be subsequently defined, rather than the whole ensemble. If the optimal damping for this ground motion violates constraints of other records in the ensemble, additional ground motions are added one at a time until an optimum is reached (stage 4 below).

Related to the above problem but less practical is the minimization of the maximum drift for an ensemble of realistic ground motion records subject to added damping that is smaller than a prescribed given value.

The main stages in the methodology are as follows:

stage 1. Select the "active" ground motion.

stage 2. Compute: a) a first guess for the damping vector; b) the equivalent constraint for the equivalent optimization problem (g_{max} in Eq. 2); and c) the ratio α_i, of the maximal to mean square drift for each story *i*.

stage 3. Solve the equivalent optimization problem for the active set of records using the Cutting Planes Method.

stage 4. Apply the remaining records in the ensemble on the optimal design for feasibility check.

stage 5. Evaluate g_{max} and the α_i's and go to Stage 3 if stopping criteria are not met.

Stage 6. Stop.

Since the optimization method is gradient based, for the equivalent problem to represent the original problem exactly, the gradient of the one must be proportional to the gradient of the other. When the α_i's in two consecutive optimization cycles (stages 3-5) are approximately proportional, and do not change drastically in the solution's region, one can claim that the gradients of the original and equivalent problems are proportional as well. The examples show that these conditions are met.

Stage 1: Selection of the "active" ground motion

The selection of the "active" ground motion affects the efficiency of the whole methodology and therefore, one would like to get a good selection of this first guess.

In this work, the record with the maximal spectral displacement is chosen to begin the process. The spectral displacement is evaluated for a given fundamental period (that of the structure) within the expected damping ratio range. Although the damping matrix is not a proportional one, the selection made here is justified by the examples.

Stage 2: Computation of a starting point, $\mathbf{c}_{do}$

Starting values for the dampers are achieved in two steps:

Step 1: As noted, a displacement spectrum is used to determine the "active" ground motion considered. The same displacement spectrum can be used to evaluate a first guess for Step 2 below. In the current step, a damping vector, which is proportional to the drifts of the first mode, is calculated such that the contribution of the first mode to the maximum drift would be equal to the maximum allowable drift.

Step 2: The damping vector provided in Step 1 is multiplied by a factor that is obtained using the Secant Method so as to satisfy

$$\max(\text{drift}_i) = \text{allowable drift} \tag{1}$$

where the drifts in Eq. 1 are computed from a time history analysis of the frame excited by the "active" ground motion.

As noted, the optimization is carried out for an equivalent problem. This stage, along with $\mathbf{c}_{\mathrm{do}}$, provides $g_{\max}$ and the α_i's for the first optimization cycle.

Stage 3: Solution of the equivalent optimization problem – "optimization stage"

Formulation of the equivalent optimization problem
The equivalent optimization problem is comprised of the added damping as an objective function, two inequality constraints and three equality constraints. The inequality constraints are the weighted average of mean square drifts of all the stories and size limitations on the dampers. Two equality constraints define the equations of motion and a third defines the mean square drifts. It may be formally described as:

$$
\begin{aligned}
&\text{mininimize}: \quad J = \mathbf{c}_{\mathrm{d}}{}^{\mathrm{T}} \cdot \mathbf{1} \\
&\text{subject to}: \\
&\left.\begin{aligned}
&\dot{\mathbf{x}}(t) = \mathbf{v}(t) \qquad ; \qquad \mathbf{x}(0) = \mathbf{0} \\
&\dot{\mathbf{v}}(t) = -\mathbf{M}^{-1}\mathbf{K} \cdot \mathbf{x}(t) - \mathbf{M}^{-1}\left[\mathbf{C} + \mathbf{C}_{\mathrm{d}}(\mathbf{c}_{\mathrm{d}})\right] \cdot \mathbf{v}(t) - \mathbf{b} \cdot a_{\mathrm{g}}(t) \; ; \mathbf{v}(0) = \mathbf{0} \\
&\dot{\mathbf{x}}_{\mathrm{ms}}(t) = \mathbf{A} \cdot \mathrm{D}(\mathbf{x}) \cdot \mathbf{x}(t) \; ; \mathbf{x}_{\mathrm{ms}}(0) = \mathbf{0} \\
&g_{\mathrm{f}} = \left. \frac{\mathbf{x}_{\mathrm{ms}}{}^{\mathrm{T}} \cdot \mathrm{D}(\mathbf{x}_{\mathrm{ms}})^{\mathrm{q}} \cdot \mathbf{x}_{\mathrm{ms}}}{\mathbf{x}_{\mathrm{ms}}{}^{\mathrm{T}} \cdot \mathrm{D}(\mathbf{x}_{\mathrm{ms}})^{\mathrm{q}} \cdot \mathbf{1}} \right|_{t_{\mathrm{f}}} \leq \mathrm{g}_{\max} \qquad \mathrm{q} \neq 0
\end{aligned}\right\} \forall a_{\mathrm{g}} \in \begin{matrix}\text{active} \\ \text{set}\end{matrix} \\
&0 \leq \mathbf{c}_{\mathrm{d}} \leq \mathbf{c}_{\mathrm{d,max}}
\end{aligned}
\tag{2}
$$

where $\mathbf{x}$ = the drift vector; $\mathbf{v}$ = the drift velocity vector; $\mathbf{M}$ = mass matrix; $\mathbf{K}$ = stiffness matrix; $\mathbf{C}$ = inherent damping matrix; $\mathbf{c}_{\mathrm{d}}$ = added damping vector; $\mathbf{C}_{\mathrm{d}}(\mathbf{c}_{\mathrm{d}})$ = supplemental damping matrix; $\mathbf{b}$ = location vector which defines location of the excitation; $\mathbf{x}_{ms}$ = drift mean square vector; $\mathrm{D}(\mathbf{x})$ = operator that forms a diagonal matrix whose diagonal elements are the elements of the vector $\mathbf{x}$; g_{f} = performance measure; $\mathrm{g}_{\max}$ = upper bound on g_{f}; q = an index to be determined subsequently; $\mathbf{c}_{\mathrm{d,max}}$ = maximum dampers' damping vector and "active set"= current set of ground motions. The coefficients matrix, $\mathbf{A}$, is a diagonal matrix whose diagonal components are:

$$
\mathbf{A}\left| A_{i,i} = \frac{\alpha_i}{D_{\mathrm{t}}} \left(\frac{100}{h_i} \right)^2 \right. \tag{3}
$$

Here D_{t} is the ground motion duration and h_i is the floor height. Thus, the elements of $\mathbf{x}_{ms}$ become $\alpha_i \frac{1}{D_{\mathrm{t}}} \int \left(\frac{100 x_i}{h_i} \right)^2 dt$ i.e. the mean square drift of the *i*-th floor (%) multiplied by the weight α_i. Hence g_{f} is the weighted average of the mean square drifts. When q is large, say 10, this weighted average approaches the value of the maximum weighted mean square drift of all the stories.

Although it has no effect on the optimal solution, the ground motion duration here is taken as the bracketed duration (Bolt 1969 [18]), using a threshold acceleration of 0.05g.

In order to use an efficient optimization scheme to solve Eq. 2 it is essential to derive the gradient of the inequality constraint while satisfying the equality constraints. Equation 2 has the general form of:

$$\begin{aligned} &\text{minimize } f(\mathbf{c}_\mathrm{d}) \\ &\text{subject to :} \\ &\mathbf{h}(\mathbf{c}_\mathrm{d}, \dot{\mathbf{y}}, \mathbf{y}, t) = \mathbf{0} \qquad ; \qquad \mathbf{y}(t_\mathrm{o}) = \mathbf{0} \\ &g(\mathbf{y}(t_\mathrm{f})) - g_{\max} \le 0 \end{aligned} \tag{4}$$

where $\mathbf{y} = \{\mathbf{x} \quad \mathbf{v} \quad \mathbf{x}_{\mathrm{ms}}\}^T$. The gradient of g is obtained by first writing the Hamiltonian of the following secondary optimization problem:

$$\begin{aligned} &\text{minimize } g(\mathbf{y}(t_\mathrm{f})) \\ &\text{subject to} \\ &\mathbf{h}(\mathbf{c}_\mathrm{d}, \dot{\mathbf{y}}, \mathbf{y}, t) = \mathbf{0} \qquad ; \qquad \mathbf{y}(t_\mathrm{o}) = \mathbf{0} \end{aligned} \tag{5}$$

The variation of this Hamiltonian results in a set of differential equations and boundary conditions to be satisfied when all multipliers of the variations (except $\delta_{\mathbf{c}_d}$) are equated to zero. The multiplier of the variation $\delta_{\mathbf{c}_d}$ will yield the expression for the evaluation of the gradient $\nabla_{\mathbf{c}_d} g(\mathbf{y}(t_f))$.

Optimization technique of the equivalent optimization problem
The Cutting Planes Method was chosen for the solution of the optimization problem. It is appropriate to use because of the "flat" behavior of the constraints that may be seen in Fig. 3. Other methods that were used proved less efficient.

Maximum step size: The step size proposed for the Cutting Planes Method is the total damping divided by a factor ρ. Instead of using a circle of radius r, (in the 2-dimensional space) for the step size, a square of side $\mathrm{r}/\sqrt{2}$, is used. This results in linear side constraints for the step size. In the n-dimensional space, $\mathrm{r}/\sqrt{\mathrm{n}}$ is taken in place of $\mathrm{r}/\sqrt{2}$. Hence, the side constraint on the step size becomes:

$$\Delta\mathbf{c}_{\mathrm{d},i} = \frac{r}{\sqrt{n}} = \frac{\frac{1}{\rho}\sum \mathbf{c}_{\mathrm{do},i}}{\sqrt{n}} \tag{6}$$

where n= number of added dampers, and ρ= constant.

Constraints elimination: Since the Cutting Planes Method is not appropriate for non-convex problems a modification is needed (although the problem seems to be convex for reasonable values of the damping (Fig. 3). The modification is as follows. If the nonlinear constraint is satisfied yet not active and its linear counterpart is satisfied and active, then that plane is removed from the next iteration. If not removed these linear constraints will cut the feasible region.

Stage 4: applying the whole ensemble on the optimal design for feasibility check
At this stage, a linear time history analysis is performed on the optimally damped structure for each of the remaining records in the ensemble, separately. A new candidate ground motion for consideration is the one with the largest maximum drift. It is actually added to the active set only if its maximum drift is larger than the maximum drift of the active set.

In Example 2 only two records are active. These records are easily tracked by the algorithm, and it is expected that the optimization scheme is likely to use, in general only a few of the records and not whole ensembles. Therefore, the scheme becomes practical in the sense of the computational effort.

Stage 5: Evaluation of new $g_{\max}$ and α_i 's – "redesign stage"

The α_i 's and $g_{\max}$ are re-evaluated separately for each ground motion within the active set.

Stage 6: Termination decision

Reanalysis is terminated if all of the following three conditions are met:

1. The changes in the α_i 's are lower than a small desired value.
2. The changes in $g_{\max}$ are lower than a small desired value.
3. No additional ground motion is needed.

NUMERICAL EXAMPLES

Example 1. A 2-story shear frame

In order to demonstrate the proposed methodology, and the characteristics of the optimization problem a 2-story shear frame is studied (Fig. 1). A 5% Rayleigh damping was assumed for the first and second modes. The constraint on the maximum drift was set to 0.009 m, which is 50% of the maximum drift of the bare frame. For convenience, the drifts were chosen as the degrees of freedom (DOF's). The two fundamental periods of the structure are 0.281 s and 0.115 s. The structure was excited by the record LA02 from the "LA 10% in 50 years" ground motions ensemble (Somerville *et. al.* [19]), which is the N-S component of El-Centro 1940 scaled by a factor of 2.01 downloaded from [20].

The mass, damping and stiffness matrices (drifts DOF's) to be used in Eq. 2 are:

$$\mathbf{M}=\begin{bmatrix}50 & 25\\ 25 & 25\end{bmatrix}\ \text{ton};\ \mathbf{C}=\begin{bmatrix}128.001 & 39.696\\ 39.696 & 72.107\end{bmatrix}\ \text{kN}\cdot\text{s/m};\ \mathbf{K}=\begin{bmatrix}37500 & 0\\ 0 & 25000\end{bmatrix}\ \text{kN/m} \tag{7}$$

The contribution of the dampers to the damping matrix is:

$$\mathbf{C}_{\mathrm{d}}=D(\mathbf{c}_{\mathrm{d}})=\begin{bmatrix}c_{\mathrm{d}_1} & 0\\ 0 & c_{\mathrm{d}_2}\end{bmatrix}\ \text{kN}\cdot\text{s/m} \tag{8}$$

and the vector $\mathbf{b}$ (Eq. 2):

$$\mathbf{b}=\{0 \quad 1\}^{\mathrm{T}} \tag{9}$$

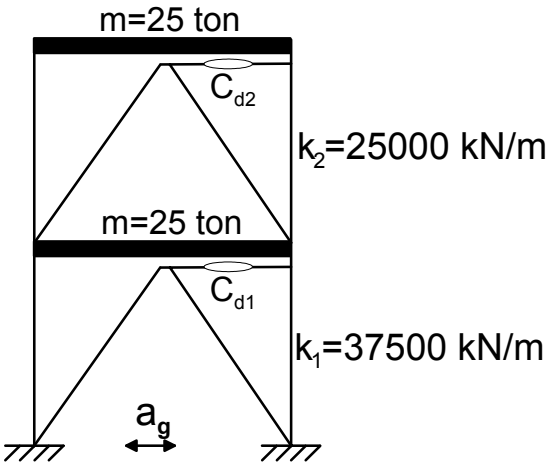

Figure 1: 2-story shear frame

The example was solved for a single record. Thus the "active" ground motion in Stage 1 is LA02. Starting values are first computed together with $g_{\max}$ and the α_i's (2nd line in Table 1). The Cutting Planes Method is then activated (Stage 3) to yield results given on the 3rd line of Table 1. The objective function, the constraint's error $(g_f - g_{\max})/g_{\max}$, and an error measure on the optimality conditions [21], are plotted against the number of iterations in Fig. 2 for the 1st optimization cycle. Also shown (Fig. 3) is a contour map of the equivalent constraint, the objective function at the optimum value (straight line) and the iterative progress towards convergence of the Cutting Planes Method. As can be seen, the constraint is close to convex. Hence the problem has only one local minimum, which is the global minimum. The "redesign stage" 5 is then performed and a 2nd optimization cycle (Stage 3) yields results that differ by 2.8% (see "normalized α_i" column of Table 1) and fall within the 3% limit set for this example.

A significant result is observed from Table 1: the maximum drift equals the maximum allowable drift in the 1st story and less than the allowable in the 2nd. Finally it might be worth noting that 7 iterations were sufficient for the first optimization cycle and only 4 were needed for the 2nd.

Table 1: Analysis results

	$c_{d,i}$		max drift [mm]		$(\mathbf{x}_{ms})_i\big\|_{t_f}$ [mm^2]		normalized α_i		g_f	max drift	J
	1	2	1	2	1	2	1	2			
bare frame	0	0	18.0	17.1	10.05	9.61	1.0	0.972	10.05	18.0	0
starting val.	1101.1	1101.1	9.1	6.7	2.08	1.11	1.0	0.998	2.08	9.1	2202.3
1st opt.	1298.3	307.4	9.0	8.1	2.09	1.98	1.0	0.928	2.09	9.0	1605.8
2nd opt.	1370.1	176.0	9.0	8.9	2.11	2.26	1.0	0.954	2.11	9.0	1546.1

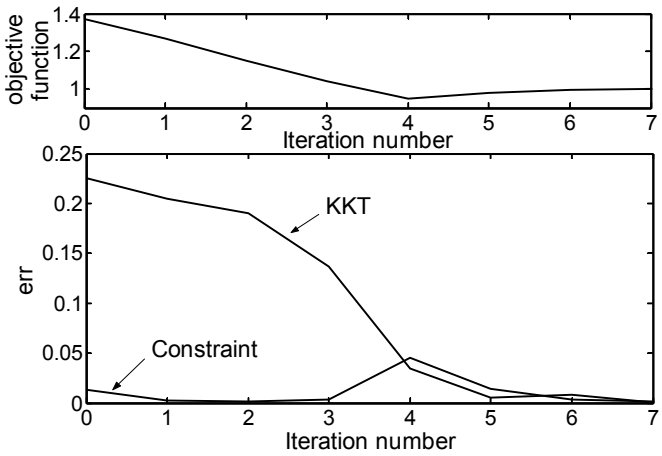

Figure 2: Convergence indicators

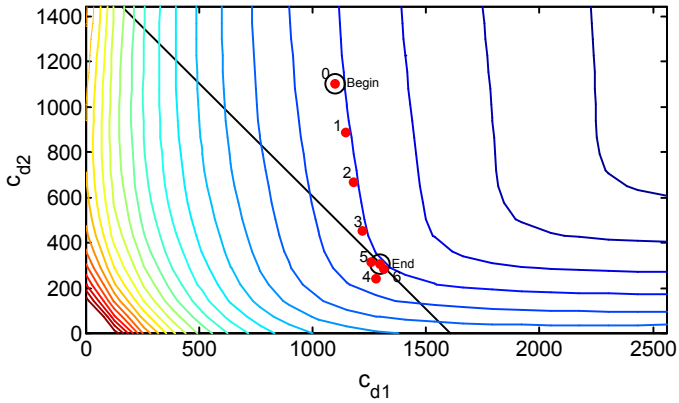

Figure 3: Convergence to optimum

Example 2. A 10-story industrial frame

In order to demonstrate the applicability of the proposed methodology to more realistic structures under an ensemble of ground motion records, an industrial building consisting of a symmetric 10-story 3-bay steel frame with inherent 2% Rayleigh damping in the first and second modes is used (Levy *et. al.* [22]). Without loss of generality, the methodology was performed on the condensed matrices neglecting axial deformations, i.e. 10 drift DOF's were used. For the sake of consistency, the axial deformations were also neglected when a full nonlinear analysis is made for verification. Design variables were assigned for each story and none were a priori, assumed equal. The ground motion ensemble was chosen as the "SE 10% in 50 years" ensemble (Somerville *et. al.* [19]) and the allowable drift was chosen as 1.0%. The record SE01 was chosen to start the process (Stage 1) since its spectral displacement for the fundamental period of the structure for all reasonable damping range had the largest value (Fig. 4). A nonlinear analysis using RUAUMOKO [23] was performed on the bare frame for this record. The resulting maximum drifts are shown in Fig 5.

Starting values (Fig. 6(a)) for the dampers were obtained using the procedure given in Stage 2, together with $g_{\max}$ and the α_i's needed for the first equivalent optimization. A linear analysis with these starting values and SE01 gives maximum drifts that are shown in Fig. 6(b). Proceeding with Stage 3, Fig. 7 is

drawn for the 1st optimization cycle and Figs. 8(a) and 8(b) show the optimal damping and maximum drifts of the damped frame excited by SE01. Stage 4 performs a linear time history analysis of the damped structure for each of the remaining 19 records. The record, SE19 led to greater maximal drifts than that of the active record, SE01 (Fig. 8(c)). Hence, this record was added to the active set. Carrying out Stage 5 the equivalent optimization problem (Stage 3) is now solved using records SE01 and SE19.

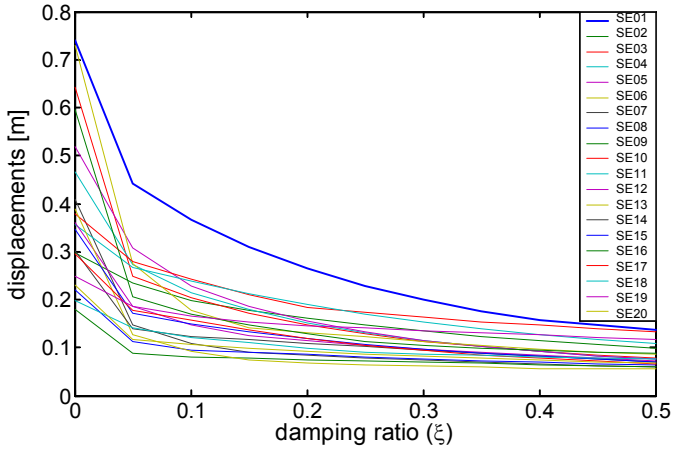

Figure 4: Spectral displacements Vs. damping ratio for the SE 10% in 50 years ensemble

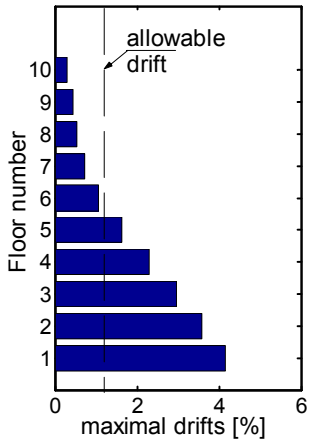

Figure 5: Maximal drifts (%) of the bare frame

After the optimal damping for these two records was calculated, a linear time history analysis was performed again on the damped structure for each of the remaining 18 records (Stage 4). This time there was no record to be added to the active set. Stage 5 was executed and the optimization cycle (Stage 3) was carried out for the third time to yield satisfactory results (within the preset tolerance of 3%). Fig. 9 shows the optimal damping and the maximum drift envelope of the damped frame using the whole ensemble.

A nonlinear time history analysis for all the records was finally performed. Although there was a slight indication of plastic hinges (maximum curvature ductility of 1.98 in several beams), the linear and nonlinear maximum response of the structure were almost identical. This validates the assumption that the damped behavior of the structure can be evaluated linearly.

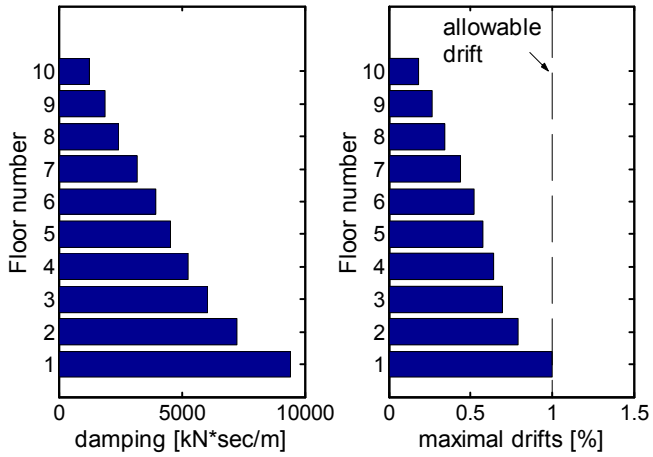

Figure 6: a) Initial supplemental damping and b) maximal drifts for initial damping and SE01

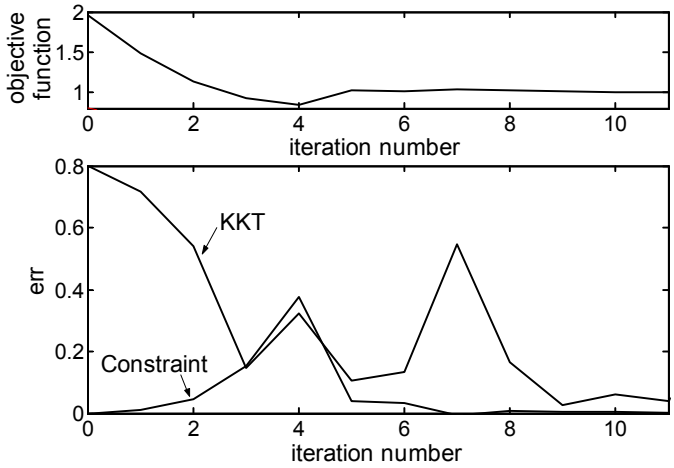

Figure 7: Convergence to optimum

It is important to emphasize that the α_i's showed small changes in the last two optimization cycles. Therefore, the equivalent optimization problem does indeed represent the original optimization problem properly. Moreover Fig. 9 shows that two drifts are fully utilized, i.e. reached the allowable drift, and the rest of the drifts are smaller than the allowable.

It is important to emphasize the fact that the records SE01 and SE19 affected the envelope drifts of different floors. Thus a design for a single record would not have been adequate. Moreover, these two records have extremely different characteristics (Fig. 10) and cannot be modeled by a random process.

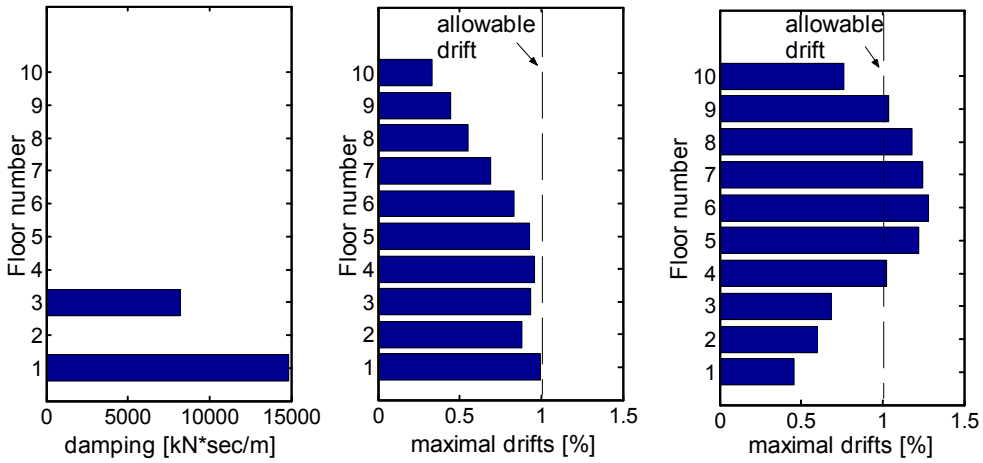

Figure 8: a) optimal damping of the damped frame for SE01; b) maximal drifts for SE01 and c) drifts envelope for the SE 10 % in 50 years ensemble

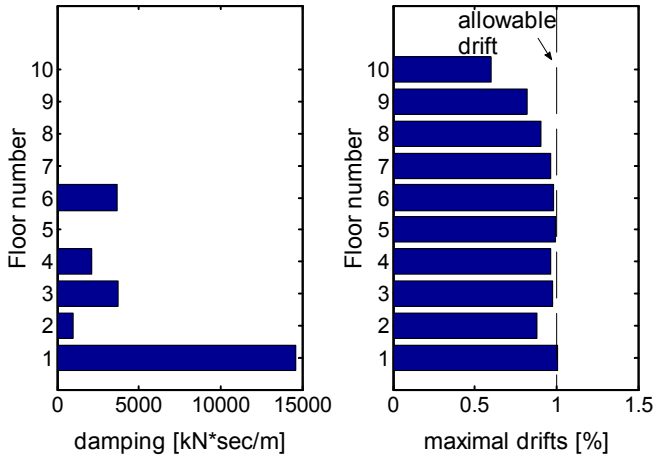

Figure 9: a) Optimal supplemental damping and b) drifts envelope for the optimally damped frame excited by the SE 10 % in 50 years ensemble

Fig. 9 indicates that using the weighted average of the mean squared drifts yields a close to uniform distribution of maximal interstory drifts, which is usually desired in structures since in this case damage (structural and nonstructural) is assumed to be uniformly distributed in the structure. An intuitive explanation is that by choosing the maximum interstory drift as a performance measure the methodology does not "spend" added damping in stories of relatively small inter story drift.

Note that the same optimal solution was achieved by using different initial starting values, so it is reasonable to assume that it is the **only** local minimum, hence, global minimum.

The optimization process for this example consisted of a total of 36 iterations and 61 time-history analyses. An additional 37 time-history analyses were needed to check for active records. The execution time of the process on a Pentium III 866 MHz personal computer lasted less than an hour using a Matlab code that was written for this purpose.

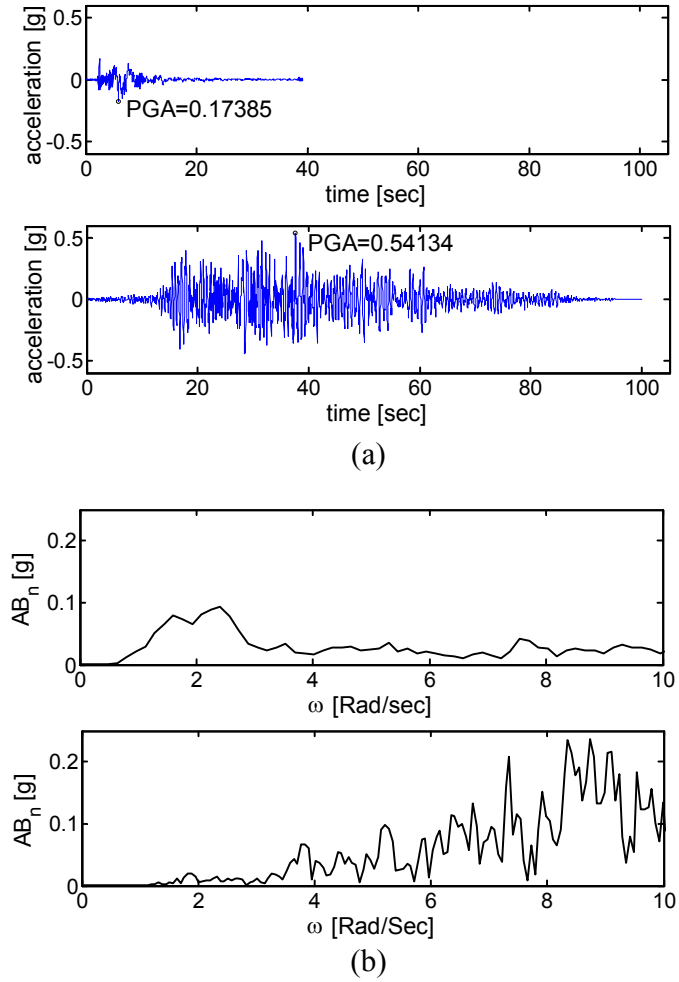

Figure 10: a) SE01 and SE19 time histories respectively and b) SE01 and SE19 Fourier spectra respectively

CONCLUSIONS

A methodology for the optimal design of added viscous damping for an ensemble of realistic ground motion records with a constraint on the maximum drift was presented. The optimization scheme allows for zero values of the design variables. Moreover, dampers of equal magnitude at specified locations may be imposed on the design process.

The optimal design yields maximum drifts that are smaller than the allowable drift. For one loading condition (one record) at least one of the maximal drifts is equal to the maximum allowable drift. For two loading conditions (two "active" records), two maximal drifts will reach the allowable (Fig. 9(b)).

Different earthquake records that are likely to be applicable in a given region, can lead to an extremely different damping distribution in the structure. Moreover, the drift envelope can be affected by more than a single record. Hence a design for an ensemble of records is essential and not a design for a single record or a design for a stochastic process.

REFERENCES

1. Soong TT, Dargush GF. *Passive energy dissipation systems in structural engineering*; Wiley: Chichester, 1997; 356 pages.
2. Miyamoto HK, Scholl RE. Case study: seismic rehabilitation of non-ductile soft story concrete structure using viscouse dampers. *Proceedings of the Eleventh World Conference on Earthquake Engineering*, Acapulco, Mexico, June 23-28, 1996, Elsevier Science Ltd; Paper No. 315.
3. Constantinou MC, Tadjbakhsh IG. Optimum design of a first story damping system. *Computers and Structures* 1983; **17** (2): 305-310.
4. Hahn GD, Sathiavageeswaran KR. Effects of added-damper distribution on the seismic response of buildings. *Computers and Structures* 1992; **43** (5): 941-950.
5. Zhang R-H, and Soong TT. Seismic design of viscoelastic dampers for structural applications. *J. of Structural Engineering* 1992; ASCE, **118** (5): 1375-1392.
6. Wu B, Ou J-P, Soong TT. Optimal placement of energy dissipation devices for three-dimensional structures. *Engineering Structures* 1997; **19** (2): 113-125.
7. Shukla AK, Datta TK. Optimal use of viscoelastic dampers in building frames for seismic force. *J. of Structural Engineering*: ASCE, 1999; **125** (4): 401-409.
8. Garcia DL. A simple method for the design of optimal damper configurations in MDOF structures. *Earthquake Spectra* 2001; **17** (3): 387-398.
9. Fu Y. Frame retrofit by using viscous and viscoelastic dampers. *Proceedings of the Eleventh World Conference on Earthquake Engineering*, Acapulco, Mexico, June 23-28, 1996, Elsevier Science Ltd; Paper No. 428.
10. Fu Y, Kazuhiko K. Comparative study of frames using viscoelastic and viscous dampers. *J. of Structural Engineering* 1998; 124, 5: 513-522.
11. Inaudi JA, Kelly JM, To CWS. Statistical linearization method in the preliminary design of structures with energy dissipating devices. ATC-17-1 1993; 509-520.
12. Gluck, N., Reinhorn, A.M., Gluck, J. and Levy, R., "Design of Supplemental Dampers for Control of Structures", *J. of Structural Engineering, ASCE,* Vol. 122, No. 12, pp. 1394-1399, Dec. 1996..
13. Takewaki I. Optimal damper placement for minimum transfer function. *Earthquake Engineering and Structural Dynamics* 1997; **26** (11): 1113-1124.
14. Takewaki I, Yoshitomi S. Effects of support stiffnesses on optimal damper placement for a planar building frame. *The Structural Design of Tall Buildings* 1998; **7**: 323-336.
15. Takewaki I, Yoshitomi S, Uetani K, Tsuji M. Non-monotonic optimal damper placement via steepest direction search. *Earthquake Engineering and Structural Dynamics* 1999; **28** (6): 655-670.
16. Singh MP, Moreschi LM. Optimal seismic response control with dampers. *Earthquake Engineering and Structural Dynamics* 2001; **30** (4): 553-572.
17. Singh MP, Moreschi LM. Optimal placement of dampers for passive response control. *Earthquake Engineering and Structural Dynamics* 2002; **31** (4): 955-976.
18. Bolt BA. Duration of strong motion. *Proceedings of the Fourth World Conference on Earthquake Engineering*, Santiago, Chile, 1969; 1304-1315.
19. Somerville P, Smith N, Punyamurthula S, Sun J. Development of ground motion time histories for Phase 2 of the FEMA/SAC steel project. *Report No. SAC/BD-97/04*, 1997.
20. Anonymous, “http://quiver.eerc.berkeley.edu:8080/studies/system/ground_motions.html”.
21. Vanderplaats, G. N. *Numerical optimization techniques for engineering design*. McGraw Hill Book Company, New York, 1984
22. Levy R, Marianchik E, Rutenberg A, Segal F. A simple approach to the seismic design of friction damped medium-rise frames. *Engineering Structures* 2001; **23** (2): 250-259.
23. Carr A. J. RUAUMOKO – Program for inelastic dynamic analysis. *Department of Civil Engineering, University of Canterbury, Christchurch*.